

## Performance of a solenoid-driven pulsed molecular beam source

L. Abad, D. Bermejo, V. J. Herrero, J. Santos, and I. Tanarro

Citation: *Rev. Sci. Instrum.* **66**, 3826 (1995); doi: 10.1063/1.1145444

View online: <http://dx.doi.org/10.1063/1.1145444>

View Table of Contents: <http://rsi.aip.org/resource/1/RSINAK/v66/i7>

Published by the [American Institute of Physics](#).

---

### Additional information on *Rev. Sci. Instrum.*

Journal Homepage: <http://rsi.aip.org>

Journal Information: [http://rsi.aip.org/about/about\\_the\\_journal](http://rsi.aip.org/about/about_the_journal)

Top downloads: [http://rsi.aip.org/features/most\\_downloaded](http://rsi.aip.org/features/most_downloaded)

Information for Authors: <http://rsi.aip.org/authors>

## ADVERTISEMENT

**For all your variable temperature, solid state characterization needs....**  
... delivering state-of-the-art in technology and proven system solutions for over 30 years!

**MMR TECHNOLOGIES**

**Solutions for Optical Setups!**

**Seebeck Measurement Systems**

**Variable Temperature Microprobe Systems**

**Hall Measurement Systems**

Email: [sales@mmr-tech.com](mailto:sales@mmr-tech.com) Web: [www.mmr-tech.com](http://www.mmr-tech.com) Phone: (650) 962-9622 Fax: (888) 522-1011

# Performance of a solenoid-driven pulsed molecular-beam source

L. Abad,<sup>a)</sup> D. Bermejo, V. J. Herrero, J. Santos, and I. Tanarro  
*Instituto de Estructura de la Materia (CSIC), Serrano 123, 28006 Madrid, Spain*

(Received 9 February 1995; accepted for publication 27 March 1995)

The characteristics of a commonly used pulsed valve for the production of free jets and molecular beams are analyzed in detail. Special attention is paid to the formation of gas pulses providing a quasisteady flow during a certain time interval within the pulse duration, and to the estimation of a scaling parameter (effective diameter) for the description of the flow field. The adequacy of this effective diameter is checked by performing time-of-flight measurements on molecular beams of Ne, N<sub>2</sub>, and CH<sub>4</sub>, and stimulated Raman spectra on free jets of N<sub>2</sub> and CH<sub>4</sub>. © 1995 American Institute of Physics.

## I. INTRODUCTION

The use of pulsed molecular-beam sources has become widespread over the last decades in many fields of research. Since the pioneering work of Hagen and co-workers<sup>1,2</sup> many types of pulsed valves have been developed.<sup>3–24</sup> The initial designs were often based on gas puffing devices for studies in plasma physics<sup>3–6,8</sup> and were then more or less modified in order to meet the specific requirements of a great variety of experiments in spectroscopy,<sup>11,18,22,25</sup> crossed beams scattering,<sup>26–30</sup> and cluster research.<sup>31–33</sup> A good review with a detailed account of the characteristics of pulsed valves, as well as a comparison of their performance with that of continuous beam sources, has been written by Gentry.<sup>34</sup>

The most obvious advantage of pulsed molecular beams is their low duty factor, which allows comparatively strong expansions and high instantaneous intensities to be reached with moderate pumping capabilities and low sample consumption. These advantages are best exploited in experiments including other pulsed elements (e.g., pulsed lasers). Nowadays gas pulses lasting for ten to several hundred microseconds are commonly used.

Practical questions concerning the performance of pulsed valves are related to the transmission of the driving pulse to the moving parts of the valve mechanism and refer to the effective opening and closing of the valve, as well as to the actual shape of the gas pulse and to its delay with respect to the driving signal. These questions depend strongly on the particular design of the different valves. A more conceptual issue related to the general operation of pulsed beam sources concerns the dynamical properties of the gas flow at different times in the pulse and, in particular, the possibility of reaching a quasisteady flow condition similar to the one occurring for continuous sources. Saenger and Fenn<sup>35,36</sup> have shown that besides the time needed for the full mechanical opening and closing of the source, a minimum time interval is required for the flow to reach a steady condition. This time interval depends on the nature of the gas and on the source parameters (i.e., pressure  $p_0$ , temperature  $T_0$ , and diameter of the source orifice,  $d$ ) and, according to

their estimates for room temperature and for values of  $p_0 d$  up to 125 mbar cm, this time interval should be at most in the tens of microseconds. Thus nonsteady flow is only likely to be a problem making difficult the theoretical predictions of the flow properties in very short gas pulses which, on the other hand, have special advantages for high-resolution experiments using time of flight (TOF) detection. This could be the case in some of the “hairpin” valves operated with a current loop such as those designed by Gentry and Giese.<sup>10,34</sup> Other experiments do not require such short pulses.

Many of the commonly used valves are based on the movement of a stem against a circular orifice. This mechanism is relatively slow and precludes in general the production of pulses shorter than 100  $\mu$ s. In this case, the attainment of a steady flow is limited by the mechanical displacement of the stem rather than by the intrinsic nonsteady flow interval and, usually, operating conditions providing a constant opening for a significant portion of the pulse can be selected. The evolution of the effective open area can be modeled in principle. Such a model has been developed recently by Zou *et al.*<sup>37</sup> and has been applied to the calculation of the total number of molecules injected into a reactor with a gas pulse. However, this simple model cannot account for the pulse shape.

A problem often encountered with this type of valve is that they do not open fully, i.e., that the effective exit area in the “full open” position is smaller than the nominal size of the orifice. This is usually due to an insufficient retreat of the closing stem. The effective opening area is then defined by the shape and by the actual position of the stem tip. Under such conditions, the real exit can differ markedly from that expected for an ideal circular sonic nozzle, for which simple theoretical expressions, relating the flow properties to the source parameters ( $p_0, T_0, d$ ), are known to be reliable. In these cases it is of particular interest to establish whether an effective size, analogous to the nozzle diameter of continuous sources and appropriate for the scaling of the flow field, can be defined from the actual opening of pulsed valves. A study of this type was carried out by Andresen *et al.*<sup>38</sup> for a commercial valve operated with a piezoelectric crystal. In this study the authors defined an effective diameter  $d_{\text{eff}}$  as that of a circle with an area identical to the actual opening and investigated the scaling of the terminal speed ratios with the product  $p_0 d_{\text{eff}}$ , which is a measure of the source Knud-

<sup>a)</sup>Present address: Universidad Alfonso X el Sabio, Villanueva de la Cañada, 28691 Madrid, Spain.

sen number. A comparison with some continuous beam results for several gases showed that the scaling with this effective diameter was correct.

In the present work, we analyze the behavior of a commonly used commercially available pulsed valve driven by means of a solenoid. This valve is handy, has compact construction, and has been adapted for different applications, which range from the generation of very cold  $\text{H}_2$  beams<sup>39</sup> to the production of radicals by pyrolysis.<sup>40</sup> Special emphasis is made in the estimation of an effective diameter related to the actual opening of the valve. In order to check the adequacy of this effective diameter as a scaling length for the flow field, we have used two different molecular properties: the evolution of the rotational temperature ( $T_{\text{rot}}$ ) of a diatomic ( $\text{N}_2$ ) and a polyatomic ( $\text{CH}_4$ ) molecule in the early stages of the supersonic expansion, and the terminal parallel speed ratio  $S_{\parallel,\infty}$  (i.e., the ratio of the flow velocity to the average thermal velocity) reached in expansions of a monatomic gas, Ne, and of the former two species,  $\text{N}_2$  and  $\text{CH}_4$ . The rotational temperatures have been determined from high-resolution stimulated raman scattering (SRS), and the velocity distributions from TOF measurements. The results are discussed and compared to current models and to experiments performed by other authors with continuous nozzles.

## II. EXPERIMENT

The valve studied in the present work is a commercial one (General Valve Corporation, series 9, rated for 12 VDC). A scheme of this valve is shown in Fig. 1(a). The exit nozzle is a small channel with two conical ends through the front plate of the valve. The shutting stem is a small Teflon cylinder (1.8 mm diameter) ending in a conical tip that fits into the nozzle channel in the closed position. The frontplate piece containing the nozzle is provided with a screw thread, and can be separated from the main body of the valve; the position of this piece must be adjusted carefully in order to get a proper operation of the shutting poppet. The nominal diameter of the circular cross section at the narrowest part of the nozzle is 0.5 mm. The outer nozzle cone has a length of 0.5 mm and a half angle of  $45^\circ$ . Such a wide cone is not expected to significantly affect the properties of the gas flow at the jet axis.<sup>31</sup> In order to perform SRS experiments closer to the actual origin of the expansion, the conical exit was removed by machining a rectangular channel 2 mm wide and 0.5 mm deep on the outer face of the frontplate. SRS and TOF measurements carried out with and without the mentioned conical exit did not show any appreciable differences. For the particular valve model we used, the electrical specifications given by the manufacturer were 12 V, 1 A for 2 ms pulses. In the present work, pulses up to 60 V and variable duration (usually around 1 ms) were used. These pulses were supplied to the valve by means of a transistor operating between cut and saturation, driven by a pulse generator. The valve was placed between the continuous voltage supply and the transistor collector. In all the experiments described here, the pulsed valve was kept at room temperature.

The valve was mounted on a movable base that could be displaced under vacuum in the  $x$ ,  $y$ , and  $z$  directions in order to allow the alignment of the molecular beams in the TOF

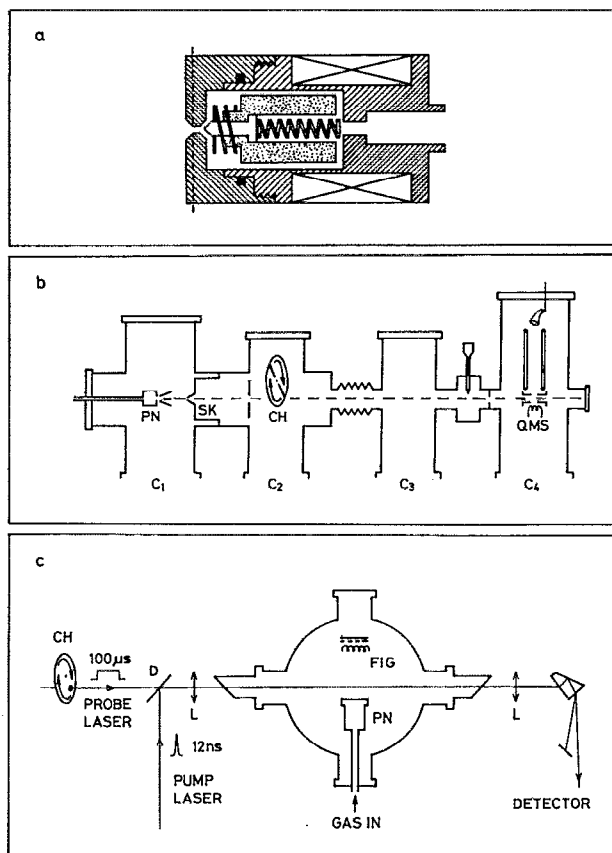


FIG. 1. (a) Scheme of the solenoid-driven pulsed molecular-beam source (not to scale). The dashed line represents the depth of the rectangular channel machined on the front of the valve in order to perform SRS measurements. (b) Experimental setup for the time-of-flight measurements. C1, C2, C3, and C4 are the vacuum chambers; PN, pulsed nozzle; SK, skimmer; CH, chopper; QMS, quadrupole mass spectrometer. (c) Arrangement used in the stimulated Raman scattering experiments. FIG, fast ionization gauge; L, lens; D, dichroic mirror.

and SRS experiments. The movement along the beam axis was achieved by means of a linear motion feedthrough provided with a micrometric screw. The precision in axial movement of the molecular-beam source is estimated to be about  $10\ \mu\text{m}$ .

The gas pulses generated from the valve were monitored by means of a fast ionization gauge (FIG) built in our laboratory according to the design of Gentry and Giese<sup>10</sup> with slight modifications. This FIG has a rise time of about  $1\ \mu\text{s}$ . Time profiles of the gas pulses were taken at a few centimeters of the exit of the valve (typically 2–8, depending on the experiment). The FIG was mounted on a movable shaft and was removed from the beam direction after the characterization of the pulses.

The experimental setup for the TOF measurements is shown in Fig. 1(b). It consists of four interconnected vacuum chambers evacuated by oil diffusion pumps. The first chamber (C1) is the one where the supersonic expansions take place; it is pumped by a  $2000\ \ell\ \text{s}^{-1}$  diffusion pump, backed by an assembly of a  $400\ \text{m}^3\ \text{h}^{-1}$  Roots pump and a  $70\ \text{m}^3\ \text{h}^{-1}$  single-stage rotary pump. This chamber was connected to the rest of the apparatus by a conical skimmer with an inner (outer) angle of  $25^\circ$  ( $32^\circ$ ) and with a circular orifice of 0.8

mm at the tip. The nozzle exit was placed at 8–10 cm from the skimmer, and the pulse frequency was made slow enough as to keep the average background pressure in the  $10^{-5}$  mbar range, in order to avoid the attenuation of the beam. The next chamber ( $C_2$ ), containing a mechanical chopper, is pumped by a  $700 \text{ } \ell \text{ s}^{-1}$  diffusion pump, and the pressure during operation is kept below  $5 \times 10^{-6}$  mbar. An additional differential pumping step is provided by the third chamber ( $C_3$ ), where the pressure is lower than  $3 \times 10^{-6}$  mbar. This chamber communicates with the detector chamber by means of a circular collimator of 3 mm diameter. The detector chamber ( $C_4$ ) is pumped with a  $300 \text{ } \ell \text{ s}^{-1}$  diffusion pump provided with a liquid-nitrogen trap. The pressure during the measurements was between  $2$  and  $7 \times 10^{-7}$  mbar. The detector for the TOF experiments was an electron bombardment quadrupole mass spectrometer provided with a secondary electron multiplier (SEM). The SEM was operated in the analog mode, and the output current was passed through a preamplifier (gain  $10^6$  V/A, rise time  $4 \text{ } \mu\text{s}$ ) and then taken to a digital oscilloscope working in the average mode. The whole mass spectrometer assembly was mounted on a 100 CF vacuum flange and placed in a cross beam configuration [see Fig. 1(b)]. The flight path  $L$  from the chopper to the detector was between 60 and 70 cm, depending on the experiment. The chopper was a rotating copper disk with a radius of 5 cm cut from a 0.25 mm thick foil and provided with two slits 1 mm wide. The chopper disk was rotated at a speed of 11 280 rpm by means of a cw electrical motor. The gate function for our experimental arrangement had a full width at half maximum of  $23 \text{ } \mu\text{s}$ . The chopper velocity was stabilized by means of an electronic servo-mechanism, based on a phase-locked loop, made in the laboratory. The deconvolution and treatment of the TOF data to obtain velocity distributions and final translational temperatures of the beams was done by using standard procedures.<sup>41</sup> In order to synchronize the chopper slit with different points of the gas pulse, a reference was taken from the chopper photodiode to the electrical pulse generator, where adequate delay between the chopper and the opening of the valve was selected.

The experimental setup for the stimulated Raman scattering was used in the stimulated Raman loss version; it has been described in detail elsewhere<sup>42,43</sup> and only a brief account will be given here. Pump and probe laser beams with parallel polarization were mixed collinearly by means of a dichroic mirror. The residual spectrum due to background gas inside the chamber was negligible for our experimental conditions. This permitted us to use this collinear configuration for probe and pump beams, allowing for a better S/N ratio and easier alignment. For  $\text{N}_2$ , however, a very broad spectrum, due to atmospheric  $\text{N}_2$  from outside the expansion chamber, along the collinear path, is superimposed to the sharp jet spectrum. In this case we used a slightly crossed configuration and performed background subtraction by pulsing the valve at half the rate of the laser shots. The laser beams were focused on the axis of the expanding jet inside the vacuum chamber by using a relatively large focal length lens,  $f=500 \text{ mm}$ . This long focal length was used in order to avoid significant broadening or shifting due to the second-order Stark effect. The probe beam was provided by a stabi-

lized  $\text{Ar}^+$  laser operating in single mode at 514 nm. The output signal had a bandwidth of less than 1 MHz and a power of about 350 mW. In order to avoid saturation of the detector, this laser beam is mechanically chopped to  $100 \text{ } \mu\text{s}$  pulses. For the pump beam, the emission of a ring dye laser operated with Rhodamine 6G was pulse amplified in a three-stage amplifier, pumped by the second harmonic of a seeded Nd:YAG laser with an extended cavity. Sulphorhodamine 640 and Kiton red were used in the amplifier for the  $\text{CH}_4$  and  $\text{N}_2$  experiments, respectively. The output of the pump laser consisted of pulses of 12 ns with a temporal and spatial Gaussian shape and with a bandwidth of  $\approx 100 \text{ MHz}$  limited by the Fourier transform of the time width of the pulses. The energy per pulse was about 7 mJ and the repetition rate 14 Hz. Laser and valve pulses were synchronized by means of a pulse generator, which allowed selection of the delay between the opening of the valve and the laser pulse. The spectroscopic signal, given by the intensity loss of the probe laser beam, is detected with a fast photodiode and acquired by means of a boxcar averager.

### III. RESULTS AND DISCUSSION

Typical time profiles of two gas pulses from the solenoid valve, recorded with the fast ionization gauge placed at 2 cm from the nozzle exit, are shown in Fig. 2(a). The two gas pulse structures correspond to the same driving voltage pulse shape (also shown), which is a square electrical signal of 1 ms duration and 60 V amplitude, but have been recorded on different days. As can be seen, in both cases the main gas pulse is wider than the driving signal, and there is a delay between the beginning of the electrical signal and the beginning of the gas pulse, due to the electrical impedance of the coil and to mechanical inertia of the moving parts. Besides the main gas pulse, other pulses due to rebounds of the closing mechanism are frequently present. These rebounds usually grow in number and intensity with an increase in the duration of the pulse. For a given electrical pulse and source pressure the rebound structure can vary within a few days of work [see lower panels of Fig. 2(a)], especially for pulses longer than 1 ms. In fact, the amount of gas entering the chamber through secondary pulses can be comparable or even greater than the amount corresponding to the first pulse. In the closed position, the valve had no appreciable leak to the expansion chamber, even for source pressures of 7 bar.

For our operative conditions (60 V) and for our particular source, gas pulses longer than about  $500 \text{ } \mu\text{s}$  lead to FIG signals of an approximately trapezoidal shape. The height of the flat pulse region does not vary with increasing duration. Shorter pulses have a rather triangular shape, and a significant intensity decrease at the maximum is observed with decreasing pulse duration. The shape and intensity of the shorter pulses can vary strongly from day to day, due conceivably to slight changes in the mechanical adjustment of the valve. For the longer pulses, this effect is not too important. For source pressures higher than 1.5–2 bar, gas pulses longer than about  $500\text{--}700 \text{ } \mu\text{s}$  are nearly square; for lower values of the source pressure these pulses have a rounder shape at the edges of the plateau.

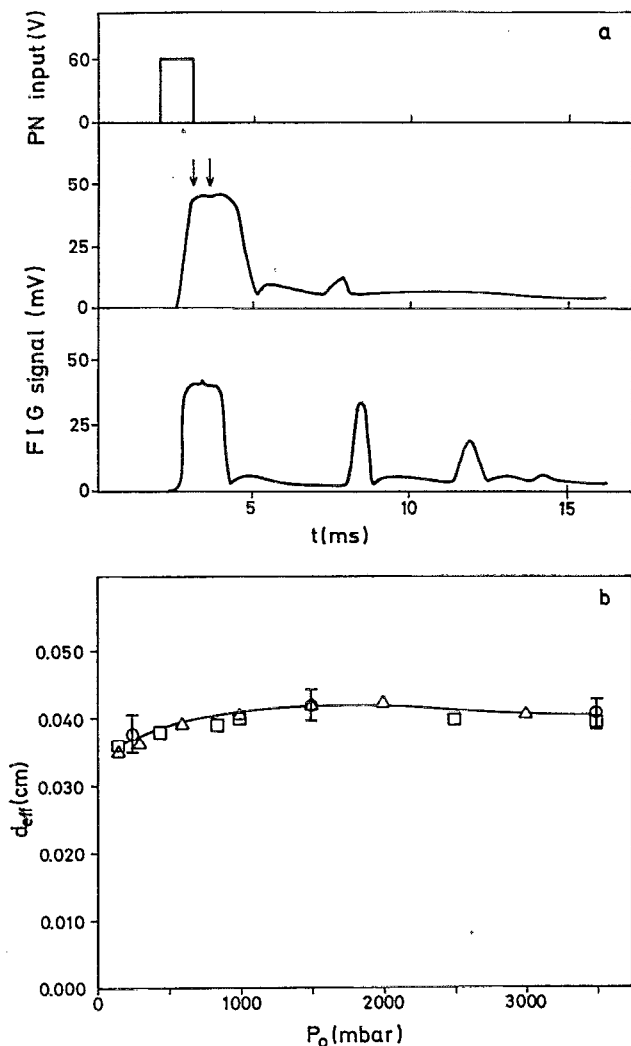


FIG. 2. (a) Voltage driving pulse of 1 ms (upper panel) and form of two gas pulse structures corresponding to this electrical signal (middle and lower panel) for a source pressure of 1500 mbar taken at different days. PN, pulsed nozzle; FIG, fast ionization gauge. Most pulses used in the present work are of the type depicted in the middle panel. The two arrows show approximately the positions where the two series of TOF and stimulated Raman-scattering measurements have been carried out (see Figs. 3 and 5). (b) Effective nozzle diameter (determined from the gas pulse shape and mass flow rate) as a function of the source pressure; the nominal nozzle diameter is 0.05 cm. Triangles and circles are measurements with  $\text{N}_2$  and squares measurements with He. The circles with error bars represent the average values of a series of 20 determinations carried out along several weeks of continued work; the error bars correspond to one standard deviation.

The flat gas pulse region is expected to correspond to a constant effective area of the source opening. In order to determine this effective area we placed the nozzle assembly and FIG in an isolated expansion chamber identical to  $C_1$ , and recorded with the FIG the pattern of gas pulses (i.e., main pulse and rebounds) for a given operation condition; we have assumed that the intensity of the signal recorded by the FIG at a given time is proportional to the actual opening of the nozzle. Then we closed the gate valve separating the expansion chamber from the diffusion pump and let the gas pulses fill the chamber (of well-known volume) up to a pressure of approximately 1 mbar. This pressure was precisely measured with a Hg compression manometer. The time

needed to reach this pressure was measured by means of a chronometer. Knowing the total amount of gas flowing into the chamber during a given time, as well as the pattern and frequency of the valve pulses, it is not difficult to estimate the effective exit area  $A_{\text{eff}}$  corresponding to the plateau region of the first peak, which is the one on which we have concentrated. Although it is not evident that the limiting exit area should have a circular shape, we have defined, in analogy with Andresen *et al.*,<sup>38</sup> an effective diameter as  $d_{\text{eff}} = (4 \times A_{\text{eff}} / \pi)^{1/2}$ , and have used this  $d_{\text{eff}}$  tentatively as a scaling length for the flow field. In most cases nitrogen was used for the determination of effective diameters; measurements with other gases led to the same results. In Ref. 38, the effective diameter of a valve driven with a piezoelectric crystal was determined by applying a voltage to the crystal and measuring the continuous gas flow through the nozzle. This procedure is not appropriate to solenoid valves if short pulses are wanted, since, in order to get small rise times, usually much higher voltages than those adequate for continuous operation are used.

For our particular pulsed valve, the estimated effective diameters are around 0.04 cm (as compared to the nominal one of 0.05 cm), and vary slightly with the source pressure [see Fig. 2(b)]. The effective openings attained with the present solenoid source are thus somewhat smaller than the nominal diameter of the exit hole. They are, however, larger than those obtained with piezoelectric valves for the same nominal diameter, as observed in Ref. 38 and in tests performed in our laboratory with an improved version of the valve mentioned in this reference. For each value of the source pressure, and for gas pulses longer than  $\approx 500 \mu\text{s}$ , the  $d_{\text{eff}}$  corresponding to the plateau of the first gas peak is almost independent of the pulse duration or frequency. This is true even in the case of complex secondary patterns, like the one shown in the lower panel of Fig. 2(a). The effective diameters thus obtained were seen to be very repetitive. In the course of tens of determinations carried out along several months, implying hundreds of thousands of shots, the  $d_{\text{eff}}$  values obtained for a given  $p_0$  never varied by more than 8%.

Time-of-flight measurements were performed on the skimmed molecular beams formed from supersonic jets of pure Ne,  $\text{N}_2$ , and  $\text{CH}_4$ . For all three gases, expansions corresponding to  $p_0 d_{\text{eff}}$  values up to 100 mbar cm were investigated. Even for the strongest expansions considered, the ratio of dimer ion to monomer ion recorded in the quadrupole mass spectrometer was less than 0.1%, and no signals corresponding to masses larger than those of dimer ions were detected.

The terminal parallel speed ratios obtained from the TOF measurements are represented in Fig. 3 as a function of the product  $p_0 d_{\text{eff}}$ . Two series of measurements were carried out at two different positions in the gas pulse: the first one 50  $\mu\text{s}$  after the beginning of the plateau region and the second one at the center of the pulse [see arrows in the middle panel of Fig. 2(a)]. It can be seen that the two series of measurements hardly differ from each other. These measurements, together with the SRS ones shown in Fig. 4, indicate that the flat region of the gas pulse actually corresponds to a quasisteady

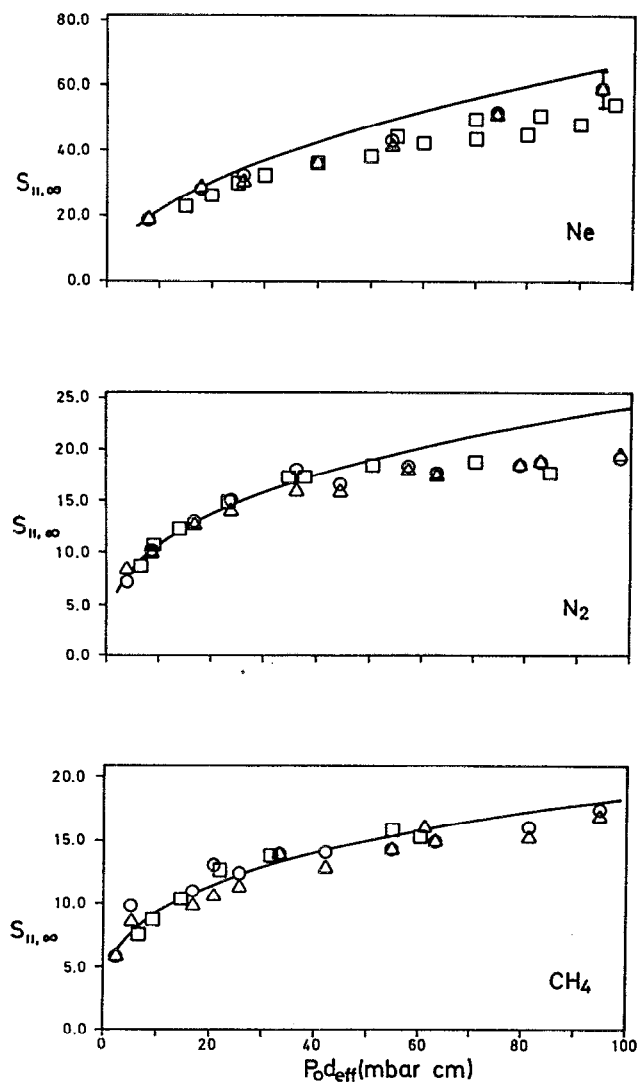


FIG. 3. Terminal parallel speed ratios of molecular beams of Ne (upper panel),  $N_2$  (middle panel), and  $CH_4$  (lower panel) as a function of  $p_0 d_{\text{eff}}$ . Circles and triangles correspond to the present pulsed beam results. The circles are measurements taken 50  $\mu\text{s}$  after the beginning of the pulse plateau and the triangles are measurements at the center of the pulse [see arrows in the middle panel of Fig. 2(a)]. The squares are the results from continuous beams reported in Refs. 46 and 47. The curves have been calculated by using the theoretical model from Ref. 44. The parameters used for  $\gamma=8/6$  (methane) have been interpolated from the ones given in Table 2.3 of the same reference.

flow, and that the quasisteady flow condition is reached shortly (at most tens of microseconds) after the beginning of the plateau region, in accordance with the results of Refs. 35 and 36.

The curves displayed in Fig. 3 correspond to the final speed ratios given by the theoretical model from Refs. 44 and 45. The values of the adiabatic coefficient ( $\gamma$ ) used in the calculations were 5/3 for Ne, 7/5 for  $N_2$ , and 8/6 for  $CH_4$ ; the last two values correspond, respectively, to linear and nonlinear molecules if one neglects the contribution of the vibrational degrees of freedom. The squares are literature results for molecular beams from continuous sources.<sup>46,47</sup> The theoretical model describes well the general evolution of

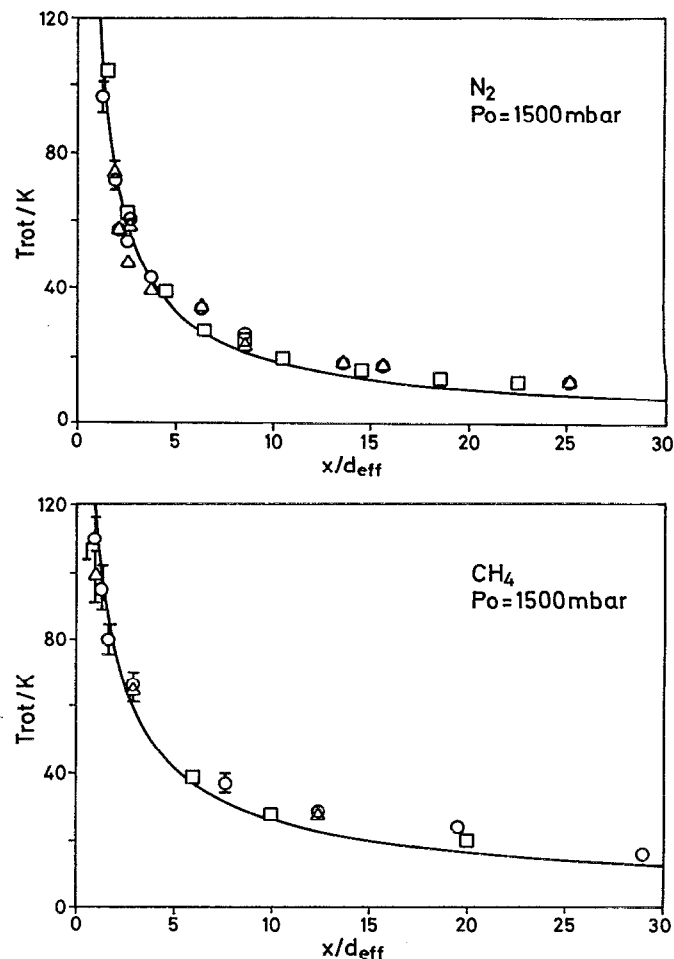


FIG. 4. Evolution of the rotational temperature in free jets of  $N_2$  (upper panel) and  $CH_4$  (lower panel). Circles and triangles have the same meaning as in Fig. 3. Squares are the results from spontaneous Raman spectra on jets from continuous nozzles (see Ref. 48). The solid curves correspond to the expected isentropic behavior (see Ref. 44) for  $\gamma=7/5$  and  $8/6$ , respectively.

the final speed ratios with the source Knudsen number and, in particular, the large differences in the values of  $S_{||,\infty}$  for mono- and polyatomic gases; however, the calculated final speed ratios deviate from the experimental ones by 10–15% in the cases of Ne and  $N_2$  for  $p_0 d_{\text{eff}}$  values larger than 30–40 mbar cm. In previous studies with continuous beams,<sup>46,47</sup> a similar deviation between experimental values and theoretical correlations was observed, and it was suggested that it could be due to scattering with the background gas in the expansion chamber or to interaction of the molecular beam with the skimmer. However, the good agreement of the continuous beam measurements with the present pulsed beam results, which have been obtained with a different experimental arrangement having a longer beam-skimmer distance and a lower background pressure, also suggests a possible inaccuracy of the theoretical model for large  $p_0 d_{\text{eff}}$  values.

Rotational temperatures of  $N_2$  and  $CH_4$  derived from SRS spectra, performed at different distances to the nozzle exit, are shown in Fig. 4. A source pressure of 1500 mbar was selected for these experiments. This pressure was chosen in order to have a number of collisions high enough to ensure that thermal equilibrium between the translational and rota-

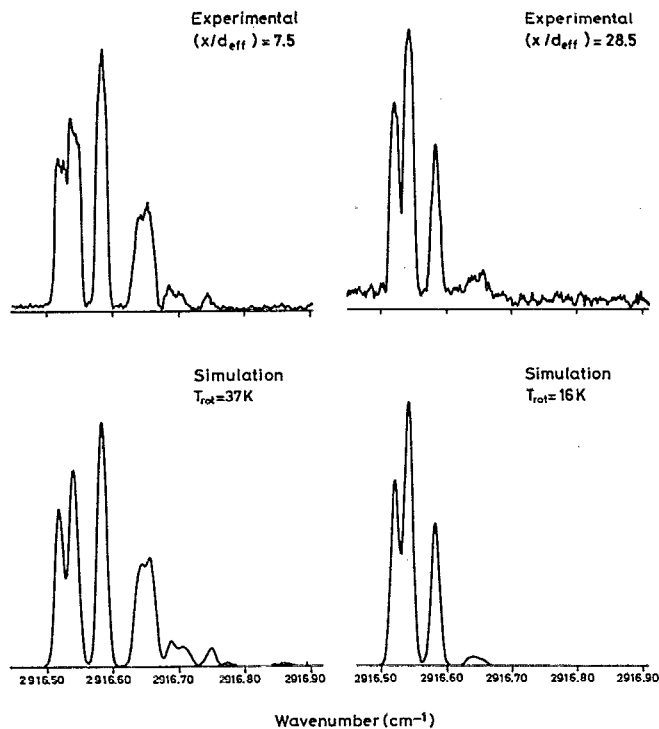


FIG. 5. Experimental and simulated SRS spectra of methane for two different distances to the nozzle exit.

tional degrees of freedom is maintained until late in the expansion. Again in this case two series of measurements have been carried out at the two positions of the gas pulse mentioned above [see Fig. 2(a)].

The spectra were recorded in the region between 2329.00 and 2330.00  $\text{cm}^{-1}$  for nitrogen (i.e., in the range of the fundamental vibrational mode) and in the region between 2916.40 and 2917.95  $\text{cm}^{-1}$  for  $\text{CH}_4$ , which corresponds to the  $\nu_1$  stretching fundamental. The SRS spectral lines are broadened by the spread of transversal velocity associated with the divergence of the jet. In the case of  $\text{N}_2$  the spectra show full rotational resolution, whereas for  $\text{CH}_4$ , especially in the measurements close to the nozzle exit, where temperature and pressure are comparatively high, some of the lines were not fully resolved. In order to simulate the spectra, it was taken into account that the proportion of the different nuclear-spin varieties of methane does not change in the course of the expansion<sup>48–50</sup> and corresponds to the one at the source (i.e., to the one at room temperature). In previous Raman and IR studies performed in  $\text{CH}_4$  jets,<sup>48,50</sup> difficulties are reported for the assignment of a Boltzmann distribution or a unique rotational temperature for the various nuclear-spin modifications. However, all of our SRS spectra, including the coldest ones where nonequilibrium effects are more likely to occur, could be satisfactorily reproduced by assuming a Boltzmann distribution of rotational levels within each nuclear-spin variety and the same temperature of the ortho-, meta-, and paramethane molecules for any given distance to the nozzle exit. As an illustration, two of the  $\text{CH}_4$  SRS spectra and their corresponding simulations are shown in Fig. 5.

The solid curves in Fig. 4 show the temperature behavior expected in an isentropic axisymmetric expansion<sup>44</sup> for  $\gamma$

values of 7/5 (upper panel) and 8/6 (lower panel). An overall good agreement with small discrepancies is found between the measurements and the isentropic curves; for large  $x/d_{\text{eff}}$  values the measured values lie slightly above the curves. No attempt has been made to use a more refined model (including, for instance, a variable  $\gamma$ ) for the comparison. The accordance is also good between the present data and the approximate temperatures derived from spontaneous Raman measurements<sup>48</sup> performed on supersonic expansions of methane and nitrogen from continuous nozzles. These expansions were stronger ( $p_0 d = 175$  mbar cm) than those of the present work, but in the absence of significant clustering, and as far as the number of collisions is high enough to maintain thermal equilibrium between translation and rotation, the same  $T_{\text{rot}}$  behavior (i.e., approximately the isentropic one) is expected for all expansions.

In the previous paragraphs we have described a procedure to estimate an effective diameter corresponding to the flat (constant intensity) region of gas pulses from a pulsed molecular-beam source. In order to check the validity of the estimated effective diameter, terminal parallel speed ratios (which depend on  $p_0 d_{\text{eff}}$  and on  $\gamma$ ) in molecular beams of Ne,  $\text{N}_2$ , and  $\text{CH}_4$ , and rotational temperatures (which depend on  $x/d_{\text{eff}}$  and on  $\gamma$ ) in free jets of  $\text{N}_2$  and  $\text{CH}_4$ , have been measured at two positions in the pulse. These measurements have provided a set of diverse dependences for  $d_{\text{eff}}$  (see Figs. 3 and 4). The results of the measurements show that the plateau region of the gas pulse corresponds to a quasisteady flow, and the comparison of the present data with other from continuous nozzles demonstrates that the effective diameter calculated from the estimated opening area is indeed adequate as a characteristic length for the scaling of the flow field.

## ACKNOWLEDGMENTS

We are indebted to J. Rodriguez for the construction of the valve driver and fast ionization gauge used in this work. We would also like to thank Dr. J. Aoiz for his careful reading of the manuscript. This work was financed by the DGI-CYT of Spain under Grants No. PB91-0128 and No. PB92-0219-C03.

<sup>1</sup>O. F. Hagena, *Z. Angew. Phys.* **16**, 183 (1963); **17**, 542 (1964).

<sup>2</sup>K. Bier and O. F. Hagena, *Rarefied Gas Dynamics: Proceedings of the 4th International Symposium*, edited by J. H. de Leeuw (Academic, New York, 1965), Vol. II, p. 260.

<sup>3</sup>N. Inoue and T. Uchida, *Rev. Sci. Instrum.* **39**, 1461 (1968).

<sup>4</sup>I. Henins and J. Marshal, *Rev. Sci. Instrum.* **40**, 875 (1969).

<sup>5</sup>G. Kuswa, C. Stallings, and A. Stamm, *Rev. Sci. Instrum.* **41**, 1362 (1970).

<sup>6</sup>B. Novak and S. Pekarek, *Rev. Sci. Instrum.* **41**, 369 (1970).

<sup>7</sup>J. A. Riley and C. F. Giese, *J. Chem. Phys.* **53**, 146 (1970).

<sup>8</sup>M. Inutake and K. Kuriki, *Rev. Sci. Instrum.* **43**, 1670 (1972).

<sup>9</sup>K. A. Köhler, *Rev. Sci. Instrum.* **44**, 73 (1973).

<sup>10</sup>W. R. Gentry and C. F. Giese, *Rev. Sci. Instrum.* **49**, 595 (1978).

<sup>11</sup>M. G. Liverman, S. M. Beck, D. L. Monts, and R. E. Smalley, *J. Chem. Phys.* **70**, 192 (1979).

<sup>12</sup>F. M. Behlen, N. Mikami, and A. S. Rice, *Chem. Phys. Lett.* **60**, 364 (1979).

<sup>13</sup>C. E. Otis and P. M. Johnson, *Rev. Sci. Instrum.* **51**, 1128 (1980).

<sup>14</sup>A. Auerbach and R. McDiarmid, *Rev. Sci. Instrum.* **51**, 1273 (1980).

<sup>15</sup>R. L. Byer and M. D. Duncan, *J. Chem. Phys.* **74**, 2174 (1981).



- <sup>16</sup>T. E. Adams, B. H. Tockney, J. S. Morrison, and E. R. Grant, *Rev. Sci. Instrum.* **52**, 1469 (1981).
- <sup>17</sup>D. Bassi, S. Iannotta, and S. Nicolini, *Rev. Sci. Instrum.* **52**, 8 (1981).
- <sup>18</sup>A. Amirav, U. Even, and J. Jortner, *Chem. Phys. Lett.* **83**, 1 (1981).
- <sup>19</sup>J. B. Cross and J. J. Valentini, *Rev. Sci. Instrum.* **53**, 38 (1982).
- <sup>20</sup>T. Imasaka, T. Okamura, and N. Ishibasi, *Anal. Chem.* **58**, 2152 (1986).
- <sup>21</sup>D. Bihat, O. Chesnovsky, U. Even, N. Lavie, and Y. Magen, *J. Phys. Chem.* **91**, 2460 (1987).
- <sup>22</sup>C. M. Lovejoy and D. J. Nesbitt, *Rev. Sci. Instrum.* **58**, 807 (1987).
- <sup>23</sup>H. M. Pang and D. L. Lubman, *Rev. Sci. Instrum.* **59**, 2460 (1988).
- <sup>24</sup>L. Li and D. L. Lubman, *Rev. Sci. Instrum.* **60**, 499 (1989).
- <sup>25</sup>F. Huiskens and T. Pertsch, *Appl. Phys. B* **41**, 173 (1986).
- <sup>26</sup>W. R. Gentry and C. F. Giese, *Phys. Rev. Lett.* **39**, 1254 (1977).
- <sup>27</sup>G. Hall, K. Liu, M. J. McAuliffe, C. F. Giese, and W. R. Gentry, *J. Chem. Phys.* **84**, 1402 (1986).
- <sup>28</sup>S. A. Buntin, C. F. Giese, and W. R. Gentry, *Chem. Phys. Lett.* **168**, 513 (1990).
- <sup>29</sup>R. E. Continetti, B. Balko, and Y. T. Lee, *J. Chem. Phys.* **93**, 5719 (1990).
- <sup>30</sup>L. Schnieder, K. Seekamp-Rahn, F. Liedeker, H. Steuwe, and K. H. Welge, *Faraday Discuss. Chem. Soc.* **91**, 259 (1991).
- <sup>31</sup>O. F. Hagena and W. Obert, *J. Chem. Phys.* **56**, 1793 (1972).
- <sup>32</sup>H. D. Barth and F. Huiskens, *J. Chem. Phys.* **87**, 2549 (1987).
- <sup>33</sup>F. Luo, G. C. McBane, G. Kim, C. F. Giese, and W. R. Gentry, *J. Chem. Phys.* **98**, 3564 (1993).
- <sup>34</sup>W. R. Gentry, in *Atomic and Molecular Beam Methods*, edited by G. Scoles (Oxford University, New York, 1988), Vol. 1, p. 54.
- <sup>35</sup>K. L. Saenger, *J. Chem. Phys.* **75**, 2467 (1981).
- <sup>36</sup>K. L. Saenger and J. B. Fenn, *J. Chem. Phys.* **79**, 6043 (1983).
- <sup>37</sup>B. S. Zou, M. P. Dudkovic, and P. L. Mills, *Rev. Sci. Instrum.* **64**, 3492 (1993).
- <sup>38</sup>P. Andresen, M. Faubel, D. Haeussler, G. Kraft, H. W. Luef, and J. G. Skofronick, *Rev. Sci. Instrum.* **56**, 2038 (1985).
- <sup>39</sup>E. Wrede, Diplomarbeit, Fakultät für Physik, Universität Bielefeld, 1993.
- <sup>40</sup>D. W. Kohn, H. Clauber, and P. Chen, *Rev. Sci. Instrum.* **63**, 4003 (1992).
- <sup>41</sup>D. J. Auerbach, in *Atomic and Molecular Beam Methods*, edited by G. Scoles (Oxford University, New York, 1988), Vol. 1, p. 362.
- <sup>42</sup>D. Bermejo, J. Santos, P. Cancio, J. L. Domenech, C. Domingo, J. M. Orza, J. Ortigoso, and R. Escribano, *J. Raman Spectrosc.* **21**, 197 (1990).
- <sup>43</sup>J. Santos, P. Cancio, J. L. Domenech, J. Rodriguez, and D. Bermejo, *Laser Chem.* **12**, 53 (1992).
- <sup>44</sup>D. R. Miller, in *Atomic and Molecular Beam Methods*, edited by G. Scoles (Oxford University, New York, 1988), Vol. 1, Chap. 2.
- <sup>45</sup>H. C. W. Beijerinck and N. F. Verster, *Physica* **111C**, 327 (1981).
- <sup>46</sup>G. Brusdeylins and H. D. Meyer, *Rarefied Gas Dyn., Proc. Int. Symp.* **11**, 919 (1979).
- <sup>47</sup>K. H. Kohl, Diplomarbeit, Universität Göttingen, 1979.
- <sup>48</sup>G. Luijks, S. Stolte, and J. Reuss, *Chem. Phys.* **62**, 217 (1981).
- <sup>49</sup>J. J. Valentini, P. Esherick, and A. Owyong, *Chem. Phys. Lett.* **75**, 590 (1980).
- <sup>50</sup>M. Hepp, G. Winnewisser, and K. M. T. Yamada, *J. Mol. Spectrosc.* **164**, 311 (1994).